Transverse mass distributions in central heavy-ion collisions at high energies*

XIE Wen-Jie(谢文杰)[1;1)] YANG De(杨德)[1] WANG Cui-Ping(王翠平)[2] WANG Zhi-Gang(王志刚)[3]

[1] Department of Physics, Yuncheng University, Yuncheng 044000, China
[2] Department of Mathematics and Physics, Hebei Institute of Architecture and Civil Engineering, Zhangjiakou 075000, China
[3] Institute of High Energy Physics, CAS, Beijing 100049, China

Abstract: The transverse mass spectra of protons, pions, kaons, Lambda and Antilambda produced in central nucleus-nucleus collisions at high energies are described by using one-temperature and two-temperature emission pictures. The calculated results are compared and found to be in good agreement with the experimental data of the E895, E866 and E917 Collaborations measured in central Au-Au collisions at the Alternating Gradient Synchrotron (AGS) energies and the NA49 Collaboration measured in central Pb-Pb collisions at the Super Proton Synchrotron (SPS) energies. It is demonstrated that the transverse mass distributions of protons, kaons, Lambda and Antilambda, except for Lambda hyperons produced in central Pb-Pb collisions at 158 A GeV, can be described by using the one-temperature emission picture, and for pions, we need to use the two-temperature emission picture.

Key words: transverse mass spectra, one-temperature emission picture, two-temperature emission picture, heavy-ion collisions

PACS: 25.75.-q, 25.75.Dw, 24.10.Pa **DOI:** 10.1088/1674-1137/35/4/007

1 Introduction

One of the main aims of relativistic heavy-ion interactions is to explore the properties of nuclear matter under extremely high temperature and high density [1]. A great body of experimental data has been reported by now [2–9]. Meanwhile, many theoretical models have been proposed to explain those experimental results [10–19]. Explanation of the transverse mass distributions of hadrons produced in heavy-ion collisions has become one of the most difficult jobs [20–22].

A two-temperature emission picture has been used to describe the high-energy nucleus-emulsion collisions processes [23]. The two emission sources are the projectile spectator contact layer with high temperature and the other part with low temperature. We can see that the two–temperature emission picture in Ref. [23] is based on the nuclear geometry model.

In the present work, we use the one-temperature and two-temperature emission pictures based on the two-source model [24, 25] and the picture of hadronic resonance decays to describe the transverse mass distributions of protons, kaons, pions, Lambda and Antilambda produced at the midrapidity in central heavy-ion collisions at energies of $E_{\rm lab}$=2–160 A GeV. The calculated results are compared with the experimental data in the range from Alternating Gradient Synchrotron (AGS) to Super Proton Synchrotron (SPS) incident energies.

2 The one-temperature and two-temperature emission pictures

According to the two-source model [24, 25], two participant fireballs are assumed to be formed in high-energy nucleus-nucleus collisions, namely a projectile fireball and a target fireball. In a high-energy hadron-hadron collision, the incident hadron collides with the

Received 5 August 2010

∗ Supported by National Natural Science Foundation of China (10975095) and Natural Science Foundation of Shanxi Province (2007011005)

1) E-mail: wenjiexie@yeah.net

target and they penetrate each other. Then a projectile fireball and a target fireball are formed and they move along the inverse beam directions. In high-energy nucleus-nucleus collisions, a lot of incident nucleons and target nucleons collide with each other, then many projectile fireballs and target fireballs are produced. We regard the projectile fireballs formed in nucleus-nucleus collisions as a big projectile fireball $P'$and these fireballs are estimated to be in thermal equilibrium at the time of freeze-out. Similarly, we regard the target fireballs formed in nucleus-nucleus collisions as a big target fireball T' and these are estimated to be in thermal equilibrium at the time of freeze-out. In the fragmentation region, the emission from the projectile fireball P' and the target fireball T' is assumed to be isotropic in emission source rest frame.

We establish a three-dimensional rectangular coordinate system and let the beam direction and the reaction plane be the Oz axis and xOz plane, respectively. As in Maxwell's ideal gas model, the three components of particle momentum in the emission source rest frame are assumed to obey Gaussian distribution having the same width. According to Refs. [26–29], the transverse momentum distribution of particles produced in the emission source i is given by

$$f_{p_{\rm T}}(p_{\rm T},\sigma_i)=\frac{p_{\rm T}}{\sigma_i^2}\exp\left(-\frac{p_{\rm T}^2}{2\sigma_i^2}\right). \tag{1}$$

Then, the transverse mass distribution of particles produced in the emission source i can be given by

$$f_{m_{\rm T}}(m_{\rm T},\sigma_i)=\frac{m_{\rm T}}{\sigma_i^2}\exp\left(-\frac{m_{\rm T}^2-m_0^2}{2\sigma_i^2}\right). \tag{2}$$

Let T stand for the temperature of emission source, and the relationship between σ_i and T is [30–32]

$$\sigma_i^2=mT=\bar{\gamma}m_0T, \tag{3}$$

where $\bar{\gamma}$, m and m_0 are the mean value of the Lorentz factor, the mass of the particles produced and the rest mass of particles, respectively. Because the excitation degree of the emission source in the relativistic heavy-ion collisions is very high, the relativistic effect cannot be neglected. Therefore, we have to take m as the moving mass in the discussion of the temperature of the emission source. In the emission source rest frame, the Lorentz factors of each particle produced are different, so we take the mean value of the Lorentz factor. We have [33]

$$\bar{\gamma}\approx\bar{E}/m_0\approx\bar{p}/m_0, \tag{4}$$

where $\bar{E}$ and $\bar{p}$ are the mean energy and the mean momentum. According to the above discussion, we know that the momentum of the particle produced in the emission source rest frame has a Maxwell distribution. Then we have

$$\bar{p}=\sigma_i\sqrt{8/\pi} \tag{5}$$

and

$$T\approx\sigma_i\sqrt{\pi/8}. \tag{6}$$

From expression (6), we can see that the temperature of the emission source increases with the momentum distribution width of emission source increasing. The emission sources have the same temperature when they have the same distribution width.

The projectile fireball P' and target fireball T' stay in the same excitation states for their relativity, then they have the same temperature. It is probable that the particles produced in the fireballs P' and T' interact with the leading particles. The hadronic resonance states may be formed. The particles produced in the hadronic resonance decays stay at a low excitation state and have a narrow standard deviation $\sigma_{\rm L}$ and a lower temperature. The particles produced in the nonresonance regions in the fireballs P' and T' stay at a high excitation state and have a wide standard deviation $\sigma_{\rm H}$ and a higher temperature. If hadronic resonance decays make a very small contribution to the transverse mass spectra of the concerned particles, namely we can neglect the contribution of the hadronic resonance decays to the transverse mass spectra of the concerned particles, we can utilize the one-temperature emission picture to describe the transverse mass spectra of the particles. We will use the two-temperature emission picture if hadronic resonance decays make a big contribution to the transverse mass spectra of the concerned particles produced in central heavy-ion collisions at high energies. For the one-temperature emission picture, the transverse mass distribution is contributed by two parts, the projectile fireball P' and the target fireball T', and we can utilize expression (2) to calculate the transverse mass distribution of the particles. For the two-temperature emission picture, there are three parts: the nonresonance regions in the fireball P', the nonresonance regions in the target fireball T' and the hadronic resonance decays. The transverse mass spectra of the particles can be written as

$$f_{m_{\rm T}}(m_{\rm T})=a_{\rm H}f_{m_{\rm T}}(m_{\rm T},\sigma_{\rm H})+a_{\rm L}f_{m_{\rm T}}(m_{\rm T},\sigma_{\rm L}), \tag{7}$$

where $a_{\rm H}$ denotes the contribution of the nonresonance regions in the fireballs P' and T', and $a_{\rm L}$ denotes the contribution of the hadronic resonance decays.

3 Comparison with experimental results

3.1 Protons

Figure 1 shows the transverse mass distributions, $(1/2\pi m_{\rm T})\,{\rm d}^2N/{\rm d}m_{\rm T}{\rm d}y$, of protons produced at the midrapidity in central Au-Au collisions at 2, 4, 6 and 8 A GeV. The circles are the E895 experimental data [34]. The curves represent our calculated results from expression (7) based on the two-temperature emission picture. The parameter values, obtained by fitting the experimental data, of expression (7) are shown in the figure and the χ^2-test method is used in our calculations. The dashed curves are the results of the one-temperature emission picture from expression (2) with σ=0.56(2 A GeV), 0.59 (4 A GeV), 0.60 (6 A GeV) and 0.63 GeV/c (8 A GeV). One can see that our calculated results are in good agreement with the experimental data of the E895 Collaboration [34].

The transverse mass distributions, $(1/m_{\rm T})\,{\rm d}^2N/{\rm d}m_{\rm T}{\rm d}y$, of protons at the midrapidity from central Pb-Pb collisions at 20, 30, 40, 80 and 158 A GeV are displayed in Fig. 2. The circles are the NA49 experimental data, which are taken from Refs. [35] (20 and 30 A GeV), [36] (40 A and 80 A GeV) and [37] (158 A GeV). The curves represent our calculated results from expression (7) in the framework of the two-temperature emission picture. The parameter values by fitting the experimental data are marked in the figure and the method of χ^2-testing is used in our calculations. The dashed curves show the results from expression (2) based on the one-temperature emission picture. From 20 to 158 A GeV, we take σ=0.65, 0.66, 0.68, 0.68 and 0.69 GeV/c, respectively. Once more, our calculated results are in good agreement with the NA49 experimental data [35–37].

In Figs. 1 and 2, we can see that both the two-temperature emission picture and the one-temperature emission picture describe the experimental data. The values of $\sigma_{\rm H}$ and σ increase with the incident energies increasing and the values of $\sigma_{\rm L}$ do not increase with the incident energies increasing at 80 and 158 A GeV. Based on the two-temperature emission picture, we have taken $a_{\rm H}$=0.90, $a_{\rm L}$=0.10. We can say that the transverse mass distributions of protons produced in central Au-Au collisions at AGS energies and central Pb-Pb collisions at SPS energies are not much affected by the hadronic resonance decays.

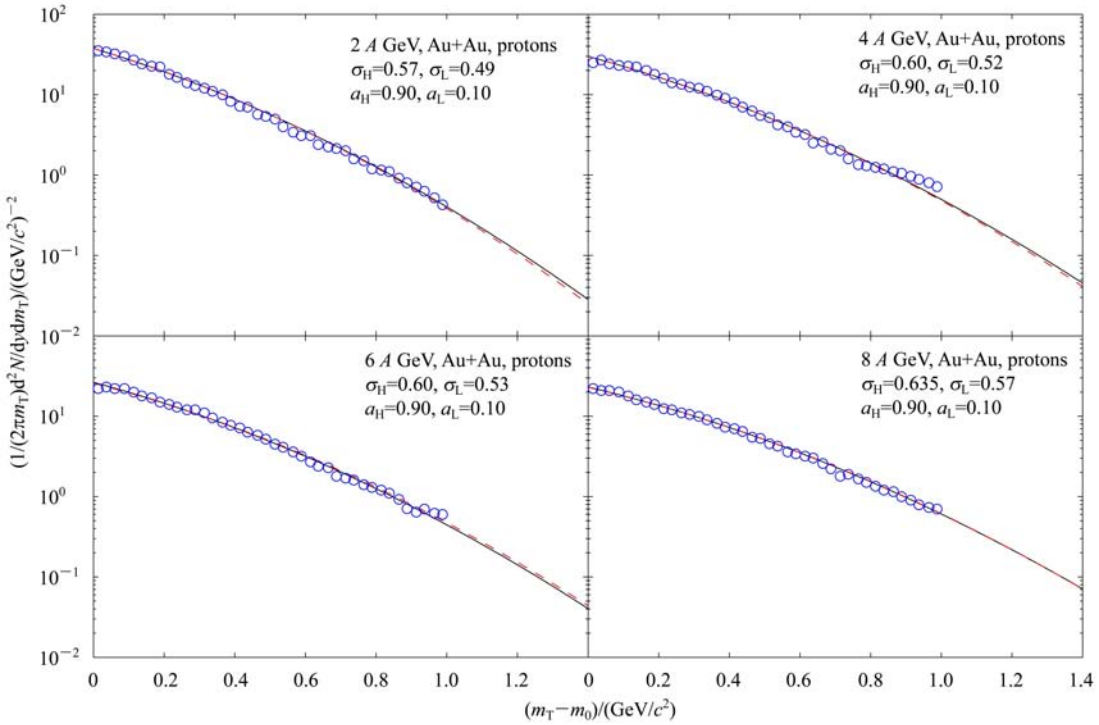

Fig. 1. The transverse mass distributions of protons at the midrapidity from central Au-Au collisions at incident energies $E_{\rm lab}$=2, 4, 6 and 8 A GeV. The circles show the E895 experimental data [34]. The curves and the dashed curves are our calculated results based on the two-temperature emission picture and the one-temperature emission picture, respectively.

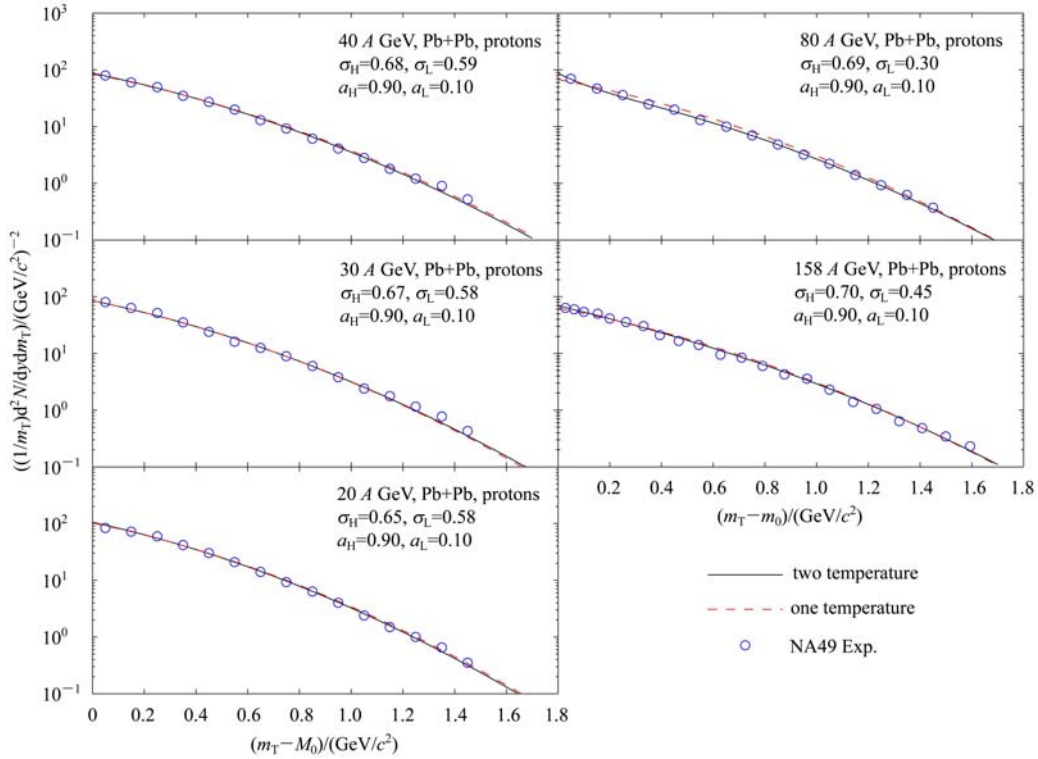

Fig. 2. The transverse mass distributions of protons at the midrapidity from central Pb-Pb collisions at incident energies $E_{\rm lab}$=20, 30, 40, 80 and 158 A GeV. The circles show the NA49 experimental data [35–37]. The curves and the dashed curves are our calculated results based on the two-temperature emission picture and the one-temperature emission picture, respectively.

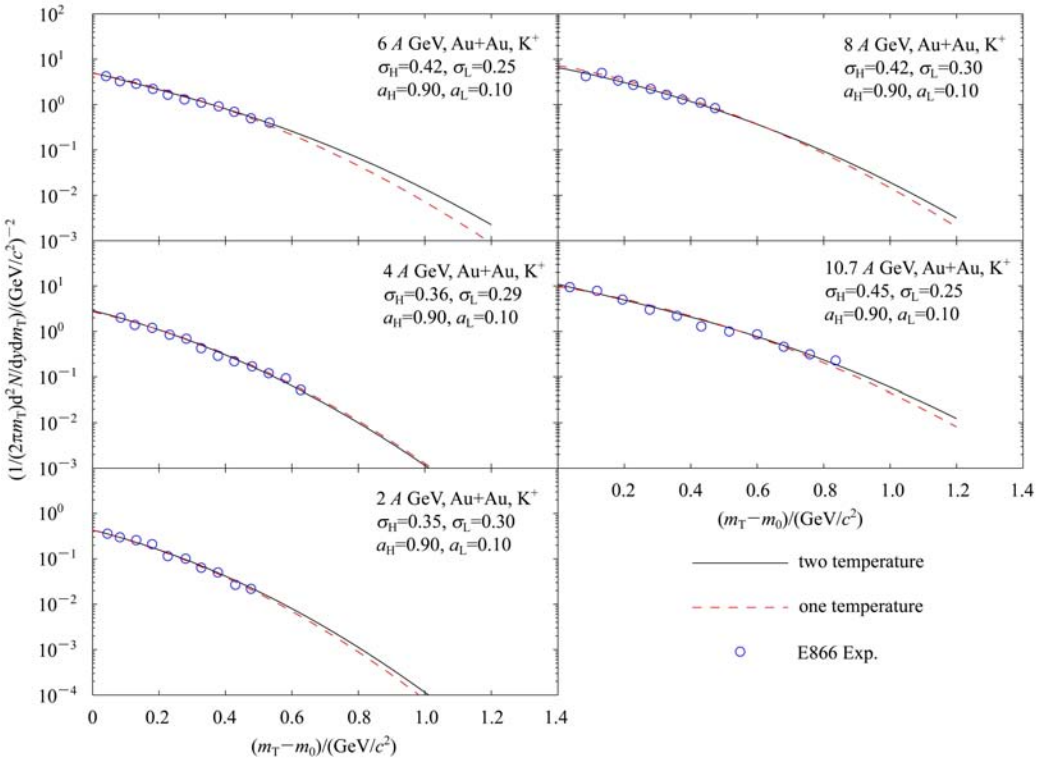

Fig. 3. The transverse mass distributions of positive kaons at the midrapidity from central Au-Au collisions at incident energies $E_{\rm lab}$=2, 4, 6, 8 and 10.7 A GeV. The circles show the E866 and E917 experimental data [38]. The curves and the dashed curves are our calculated results based on the two-temperature emission picture and the one-temperature emission picture, respectively.

3.2 Kaons

We show in Fig. 3 the transverse mass distributions, $(1/2\pi m_{\rm T})\,{\rm d}^2N/{\rm d}m_{\rm T}{\rm d}y$, of positive kaons produced at the midrapidity in central Au-Au collisions at various incident energies $E_{\rm lab}$=2, 4, 6, 8, and 10.7 A GeV. The circles represent the experimental data of the E866 and the E917 Collaborations [38]. The curves denote our calculated results by using expression (7) in the framework of the two-temperature emission picture. The parameter values obtained by fitting the experimental data are shown in the figure and the χ^2-test method is used in our calculations. The dashed curves are the result of using expression (2) with σ=0.34 (2 A GeV), 0.36 (4 A GeV), 0.39 (6 A GeV), 0.40 (8 A GeV) and 0.43 GeV/c (10.7 A GeV). The same conclusion from Fig. 3 as from Figs. 1 and 2 can be obtained. Expressions (2) and (7) describe the transverse mass spectra of positive kaons produced in central Au-Au collisions at the AGS energies.

In Fig. 4, the transverse mass distributions, $(1/m_{\rm T})\,{\rm d}^2N/{\rm d}m_{\rm T}{\rm d}y$, of positive and negative kaons produced at the midrapidity in central Pb-Pb collisions at 40, 80 and 158 A GeV are given respectively. The circles denote the experimental data of the NA49 Collaboration [39]. The curves represent our calculated results from expression (7). In the selection of parameter values, the method of χ^2-test is used. The obtained parameter values are marked in the figure. The dashed curves show the results from expression (2) and in our calculations, we take σ=0.45 (40 A GeV), 0.46 (80 A GeV), 0.46 GeV/c (158 A GeV) for negative kaons, and σ=0.48 GeV/c (40 A GeV, 80 A GeV and 158 A GeV) for positive kaons. One can see that our calculated results are in good agreement with the experimental data in central Pb-Pb collisions at SPS energies.

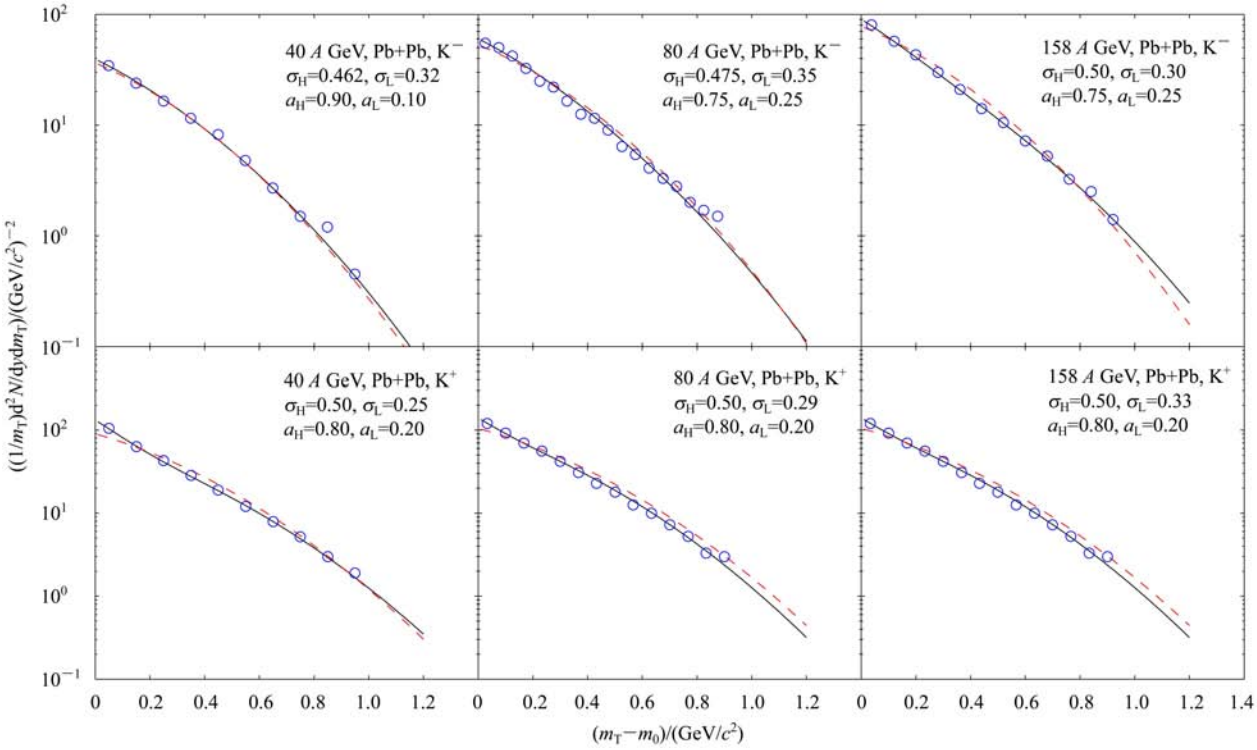

Fig. 4. The transverse mass distributions of positive and negative kaons at the midrapidity from central Pb-Pb collisions at incident energies $E_{\rm lab}$=40, 80 and 158 A GeV. The circles show the NA49 experimental data [39]. The curves and the dashed curves are our calculated results based on the two-temperature emission picture and the one-temperature emission picture, respectively.

As for protons, the contribution of the hadronic resonance decays to the transverse mass distributions of kaons at the midrapidity from central Au-Au collisions at AGS energies and central Pb-Pb collisions at SPS energies are smaller. The values of $\sigma_{\rm H}$ and σ increase with the incident energies increasing and the values of $\sigma_{\rm L}$ do not increase with the incident energies increasing.

3.3 Lambda and antilambda

Figure 5 shows the transverse mass distributions, $(1/m_{\rm T})\,{\rm d}^2N/{\rm d}m_{\rm T}{\rm d}y$, of Lambda and Antilambda hy-

perons produced at the midrapidity in central Pb-Pb collisions at 40, 80, and 158 A GeV, respectively. The circles are the NA49 experimental data [40]. The curves are our calculated results from expressions (7) and the χ^2-test method is used in the selection of parameter values. The parameter values obtained by fitting experimental data are denoted in the figure. The dashed curves are the results from expression (2) based on the one-temperature emission picture, and in our calculations we take σ=0.665 (40 A GeV), 0.69 (80 A GeV), 0.70 GeV/c (158 A GeV) for Lambda hyperons, and σ=0.76 (40 A GeV), 0.73 (80 A GeV), 0.71 GeV/c (158 A GeV) for Antilambda hyperons. The same conclusion from Fig. 5, except for Lambda hyperons at 158 A GeV, as from Figs. 1–4 can be obtained, namely expressions (7) and (2) describe the transverse mass spectra of Lambda and Antilambda hyperons produced at the midrapidity in central Pb-Pb collisions at SPS energies. The values of $\sigma_{\rm H}$ and σ increase with the incident energies increasing for Lambda hyperons, and for Antilambda hyperons, the values of $\sigma_{\rm H}$ and σ decrease with the incident energies increasing. The values of $\sigma_{\rm L}$ do not depend on the incident energies.

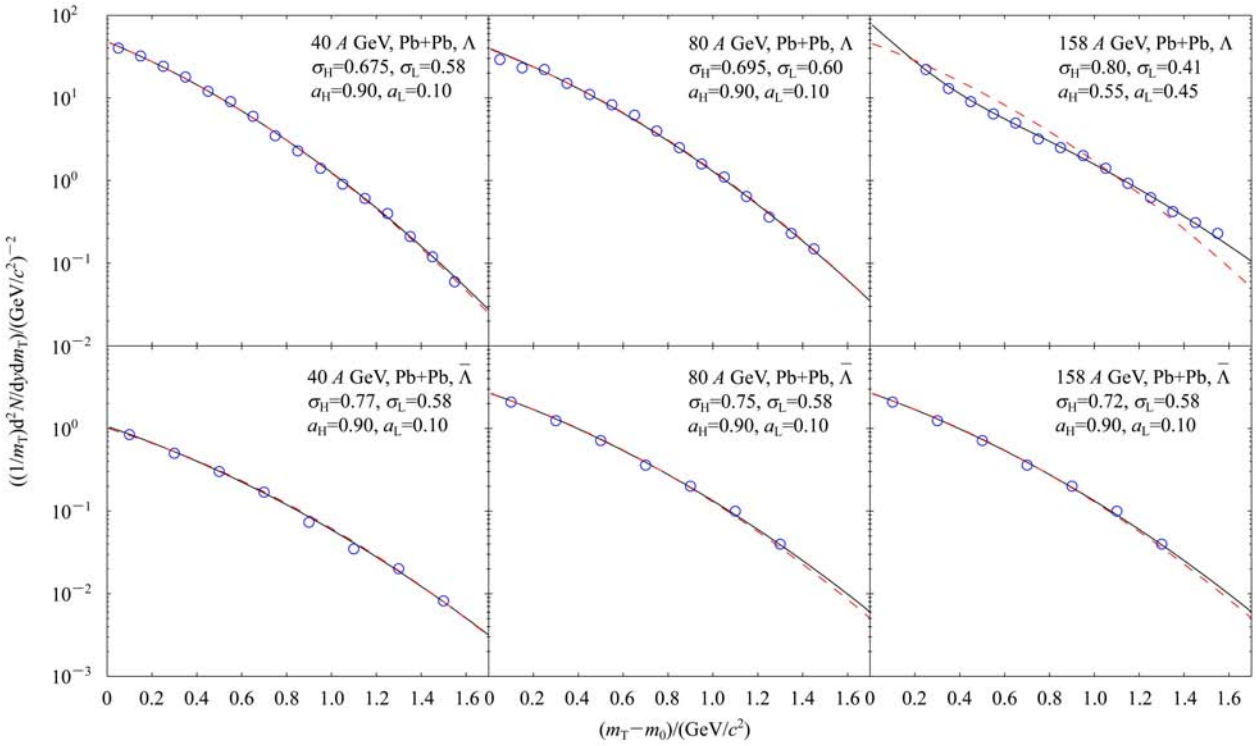

Fig. 5. The same as in Fig. 4 but for Lambda and Antilambda hyperons. Data are taken from Ref. [40].

3.4 Pions

The transverse mass distributions, $(1/2\pi m_{\rm T}){\rm d}^2N/{\rm d}m_{\rm T}{\rm d}y$, of positive pions produced at the midrapidity in central Au-Au collisions at 2, 4, 6, 8, and 10.7 A GeV are displayed in Fig. 6. The circles indicate the experimental data of the E866 and E917 Collaborations [38]. The curves represent our calculated results from expression (7) in the framework of the two-temperature emission picture. In the selection of parameter values, the χ^2-test method is used and the obtained parameter values are marked in the figure. The dashed curves denote the results from expression (2) with σ=0.26 (2 A GeV), 0.27 (4 A GeV), 0.28 (6 A GeV), 0.29 (8 A GeV), and 0.30 GeV/c (10.7 A GeV). One can see that expression (7) describes the transverse mass distributions of positive pions produced at the midrapidity in central Au-Au collisions at AGS energies.

In Fig. 7, the transverse mass distributions, $(1/m_{\rm T}){\rm d}^2N/{\rm d}m_{\rm T}{\rm d}y$, of negative pions at the midrapidity from central Pb-Pb collisions at 40, 80, and 158 A GeV are given. The circles show the NA49 experimental data [39]. The curves denote our calculated results from expression (7) based on the two-temperature emission picture. The parameter values by fitting the experimental data are indicated in the figure and the χ^2-test method is used in the selection of parameter values. The dashed curves are our calculated results from expression (2) with σ=0.25

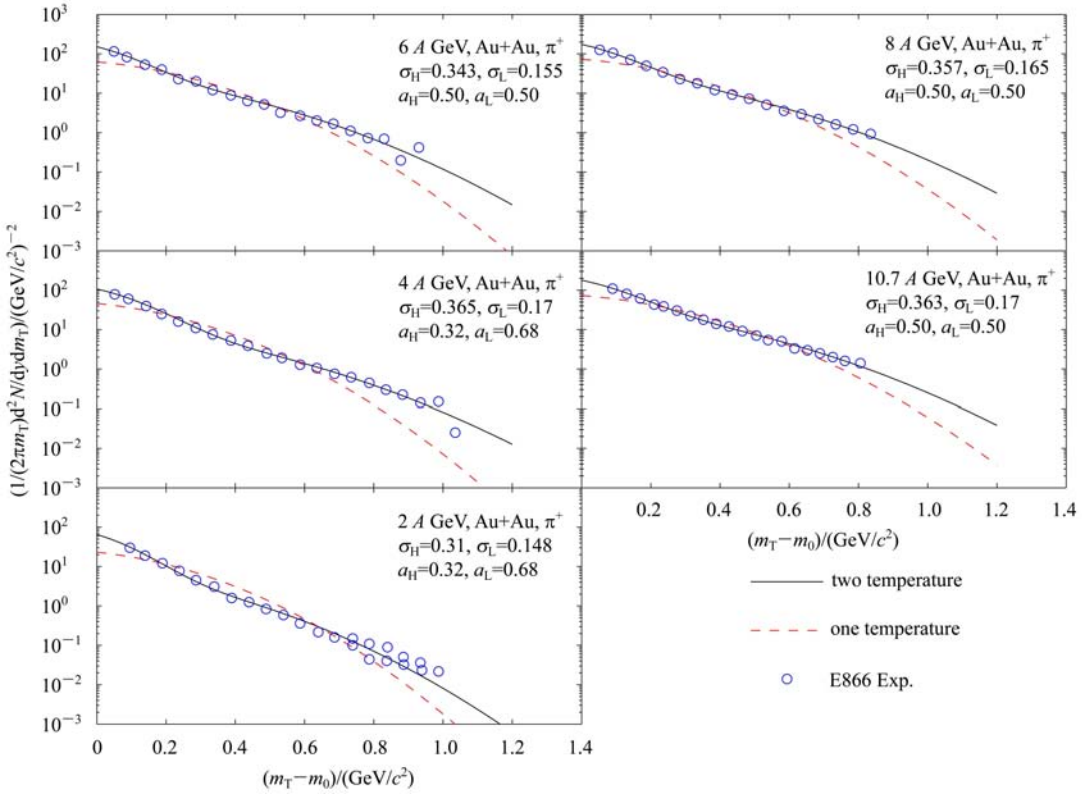

Fig. 6. The caption is the same as for that Fig. 3, but this shows the distributions of positive pions.

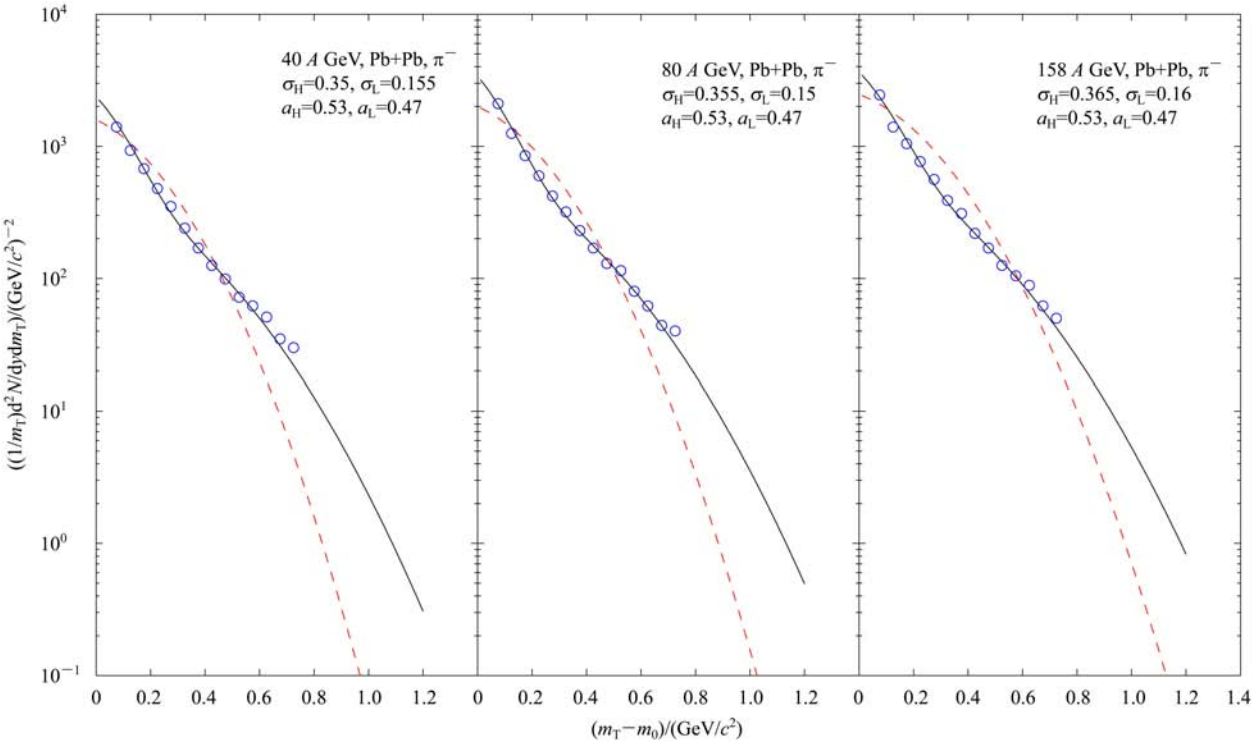

Fig. 7. As for Fig. 4, but this shows the results of negative pions.

(40 A GeV), 0.26 (80 A GeV), 0.28 (158 A GeV) based on the one-temperature emission picture. The same conclusion from Fig. 7 as from Fig. 6 can be obtained. Expression (7) describes the transverse mass distributions of negative pions produced at the midrapidity in central Pb-Pb collisions at SPS energies. The values of $\sigma_{\rm H}$ and σ increase with the incident energies increasing. The values of $\sigma_{\rm L}$ do not depend on the incident energies.

4 Conclusions and discussions

We have investigated the transverse mass distributions of protons, kaons, pions, Lambda and Antilambda produced in central heavy-ion collisions at AGS and SPS energies. Our results show that the transverse mass spectra of protons, kaons, Lambda and Antilambda, except for Lambda hyperons produced in central Pb-Pb collisions at 158 A GeV, are not much affected by the hadronic resonance decays and can be described by the one-temperature emission picture. It is different for pions as the transverse mass distributions of pions from the hadronic resonance decays have a higher proportion than that of other produced particles, and we have to use the two-temperature emission picture to describe the transverse mass distributions of pions produced at the midrapidity in central heavy-ion collisions at AGS and SPS energies.

V. Greco, et al. [41] and X. Dong, et al. [42] have supposed that the resonance decays could have a significant effect on pion production. Our calculated results show that the hadronic resonance decays have a larger contribution to the transverse mass distributions of pions. Our results seem to be consistent with the results in Refs. [41] and [42].

We can use the temperature to denote the excitation degree of emission source. According to expression (6), the momentum distribution width reflects the temperature of the emission source. From the parameter values marked in Figs. 1–7, it is found that the momentum distribution width is big for protons, Lambda and Antilambda, medium for kaons and small for pions. This indicates that the emission source temperature is high for emitting protons, Lambda and Antilambda, medium for emitting kaons and low for emitting pions. We can say that the protons, Lambda and Antilambda hyperons are emitted early, the kaons are emitted late and the pions are emitted later in the fireballs P' and T'.

References

1 Geiss J, Cassing W, Greiner C. Nucl. Phys. A, 1998, **644**: 107–138
2 Partlan M D et al. Phys. Rev. Lett., 1995, **75**: 2100–2103
3 HONG B et al. Phys. Rev. C, 2005, **71**: 034902
4 HONG B et al. Phys. Rev. C, 1998, **57**: 244–253
5 Förster A et al. Phys. Rev. Lett., 2003, **91**: 152301
6 Barrette J et al. Phys. Rev. C, 1997, **55**: 1420–1430
7 Barrette J et al. Phys. Rev. C, 2000, **63**: 014902
8 Klay J L et al. Phys. Rev. C, 2003, **68**: 054905
9 Anticic T et al. Phys. Rev. C, 2009, **79**: 044904
10 Sorge H, Stöcker H, Greiner W. Nucl. Phys. A, 1989, **498**: 567–576
11 Capella A, Sukhatme U, TAN C I et al. Phys. Rep., 1994, **236**: 225–329
12 Anderson B, Gustafson G, Pi H. Z. Phys. C, 1993, **57**: 485
13 SA B H, TAI A. Phys. Rev. C, 1997, **55**: 2010–2015
14 Ehehalt W, Cassing W. Nucl. Phys. A, 1996, **602**: 449–486
15 Bravina L V, Amelin N S, Csernai L P et al. Nucl. Phys. A, 1994, **566**: 461–464
16 Meyers W D. Nucl. Phys. A, 1978, **296**: 177–188
17 Letessier J, Rafelski J, Tounsi A. Phys. Lett. B, 1992, **292**: 417–423
18 Braun-Munzinger P et al. Phys. Lett. B, 1996, **365**: 1–6
19 Braun-Munzinger P et al. Phys. Lett. B, 1995, **344**: 43–48
20 Bratkovskaya E L et al. Phys. Rev. Lett., 2004, **92**: 032302
21 Bratkovskaya E L et al. Phys. Rev. C, 2004, **69**: 054907
22 Wagner M, Larionov A B, Mosel U. Phys. Rev. C, 2005, **71**: 034910
23 LIU F H. Chin. J. Phys., 2000, **38**: 1063–1073
24 CHANG W Y. Acta. Phys. Sin., 1961, **17**: 9–33 (in Chinese)
25 LIU F H. Nucl. Phys. Rev., 1998, **14**: 21–25 (in Chinese)
26 TANG X W, XU G F, LIU F H. Progress in Phys., 1993, **13**: 378–404 (in Chinese)
27 LIU F H, TANG X W. HEP & NP, 1994, **18**: 334–339 (in Chinese)
28 LIU F H, SUN H C. HEP & NP, 1994, **18**: 1073–1077 (in Chinese)
29 LIU F H. Europhys. Lett., 2003, **63**: 193–199
30 Goldhaber A S. Phys. Lett. B, 1974, **53**: 306–308
31 Bhalla K B, Chaudhry M, Lokanathan S et al. Nucl. Phys. A, 1981, **367**: 446–458
32 LIU F H. Chin. J. Phys., 2003, **41**: 357–371
33 MENG C R. HEP & NP, 2006, **30**: 322–326 (in Chinese)
34 Klay J L et al. Phys. Rev. Lett., 2002, **88**: 102301
35 Gazdzicki M et al. J. Phys. G, 2004, **30**: S701
36 van Leeuwenet M et al. Nucl. Phys. A, 1999, **715**: 161c–170c
37 Appelshäuser H et al. Phys. Rev. Lett., 1999, **82**: 2471–2475
38 Ahle L et al. Phys. Lett. B, 2000, **476**: 1–8
39 Afanasiev S V et al. Phys. Rev. C, 2002, **66**: 054902
40 Anticic T et al. Phys. Rev. Lett., 2004, **93**: 022302
41 Greco V, Ko C M. Phys. Rev. C, 2004, **70**: 204901
42 DONG X, Esumi S, Sorensen P et al. Phys. Lett. B, 2004, **597**: 328–332